IEEE Access
Multidisciplinary | Rapid Review | Open Access Journal

Received June 7, 2020, accepted August 2, 2020, date of publication August 10, 2020, date of current version August 21, 2020.

Digital Object Identifier 10.1109/ACCESS.2020.3015429

Increasing Surface Coating Quality Using New Generation Current Waveforms

GÜLÇIN MÜHÜRCÜ[1] AND MUSTAFA KEMAL KÜLEKCI[2]
[1]Pınarhisar Vocational School, Control and Automation Technologies, Kırklareli University, Kırklareli 39300, Turkey
[2]Mechanical Engineering Department, Faculty of Engineering, Tarsus University, Tarsus 33480, Turkey

Corresponding author: Gülçin Mühürcü (gulcinmuhurcu@klu.edu.tr)

ABSTRACT In this study, a novel current generator system was designed that can convert the basic signals used in engineering field into electrical current waves. The current generator system was realized by using Buck Converter and H-Bridge, which are Power Electronics circuit topologies. In order to produce the predicted current waveforms, the Artificial Neural Network (ANN), as a nonlinear control algorithm, has been adapted to the hybrid Power Electronics system. Then, Electrodeposition based coating experiments were carried out using the new generation current generator system. Copper (Cu) was used as a cathode and Nickel (Ni) as an anode in the coating process. Coating experiments were carried out for constant maximum current (Imax) conditions. The experiments were repeated with 3 different frequencies for each coating current wave. After coating, the surface morphology and sharp edge coating success of the covered areas were examined and the results were discussed by comparing to the DC's, PC's and PRC's.

INDEX TERMS Buck converter, H-bridge, ANN, non-linear control, current wave form, electrodeposition, coating, surface morphology, edge coating.

I. INTRODUCTION

Material interaction depends on the working conditions in industries occur first on the materials' surfaces. To be able to reduce the interactions, development for surface modification techniques has become mandatory. Surface modification techniques which are used to increase materials' life and increase materials' durability in production processes in order to comply with developing standards, have become an important engineering work area subject [1], [2]. Some of the techniques that are used to improve surface properties may be given as Physical Vapor Deposition (PVD), Chemical Vapor Deposition (CVD), Sol Gel, Thermal Spray, Micro Arc Oxidation (MAO), Ion Implantation and Electrodeposition [3]. Electrodeposition technique is one of the most economical methods used for many years to produce metallic coatings. The main target in metal coating processes by Electrodeposition method is to get better solutions on wear, corrosion and high temperature resistance and also on hardness [4]–[7]. Electrodeposition is a process that uses electrical current or potential to deposit a metal or alloy film from an electrolyte to a conductive substrate by reducing metallic ions [8]–[10]. Here, electrical current is very important parameter that affects too much the coating success [11], [12].

In Electrodeposition method it's widely used Direct Current (DC) for the production of metallic coatings [13], [14]. In recent years, in addition to DC there are used Pulse Current (PC) and Pulse Reverse Current (PRC) Electrodeposition methods for coating processes [12], [15]–[25]. Ni and its alloys are also widely used in this deposition area due to their healing properties at various values such as good corrosion, good wear resistance and high hardness [26], [27]. In Electrodeposition coating process that is applied with PC or PRC, it has been shown that changing the pulse width of current it may affect the coating results positively [28].

PC and PRC Electrodeposition coating methods are presented in various research articles that they are more successful than DC coating method. In this study, in addition to these three electrical current waveforms, the answer to the question of whether the values on the coating parameters of the currents with additional different waveforms can be improved had been searched. For this, computer controlled current source hardware was developed. The technological infrastructure of the current source system was based on Software, Power Electronics and nonlinear control science based on ANN. The results were discussed by making

The associate editor coordinating the review of this manuscript and approving it for publication was Her-Terng Yau.

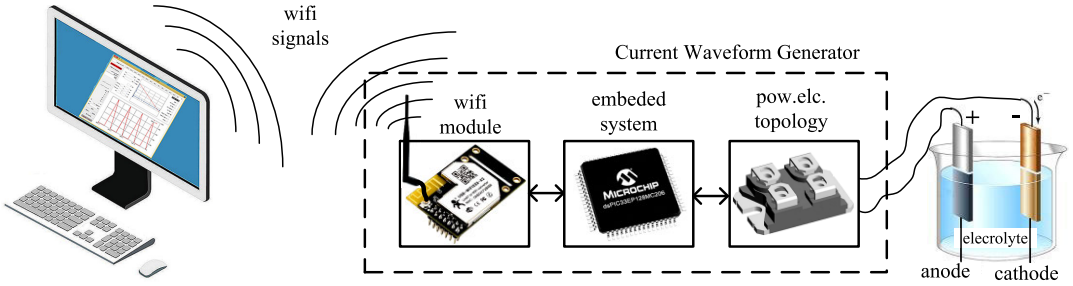

FIGURE 1. Working style of current waveform generator.

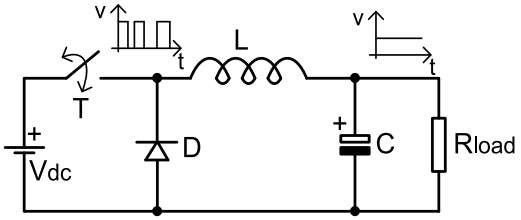

FIGURE 2. Buck Converter topology.

Ni plating on Cu with various current waveforms with different rate of changes.

II. CURRENT WAVEFORM GENERATOR SYSTEM

The current waveform generator system consists of three design sections: computer software, power electronics circuit topology and embedded system. The embedded system is arranged in order to control the operation of circuit elements belonging to the power electronics topology and to operate the user requests created through the PC software. Data communication between the PC software and the embedded system is carried out using the WiFi (wifi232) communication module, Figure 1.

A. POWER ELECTRONICS CIRCUIT TOPOLOGY

The resistance (Rload) of the electrolyte in the coating process is in the order of mΩ. The current generator is designed to deliver up to 10 amps. Considering the highest current value that the device can produce and low electrolyte resistance, it had envisaged that the busbar voltage value of the generator is enough to be DC 10V as given in (1).

$$\mathbf{V} = \mathbf{I} * \mathbf{R} \tag{1}$$

In the coating process, the voltage to be given to the electrolyte must be adjusted so that the parameter values of the current flowing from the electrolyte and the reference current are matched with each other. In order to meet this condition, the busbar voltage must somehow be converted to the lower voltage levels needed. Therefore, in order to transfer energy to load resistance at low voltage levels [29], [30], this study uses power electronics switched circuit topology called Buck Converter, Figure 2.

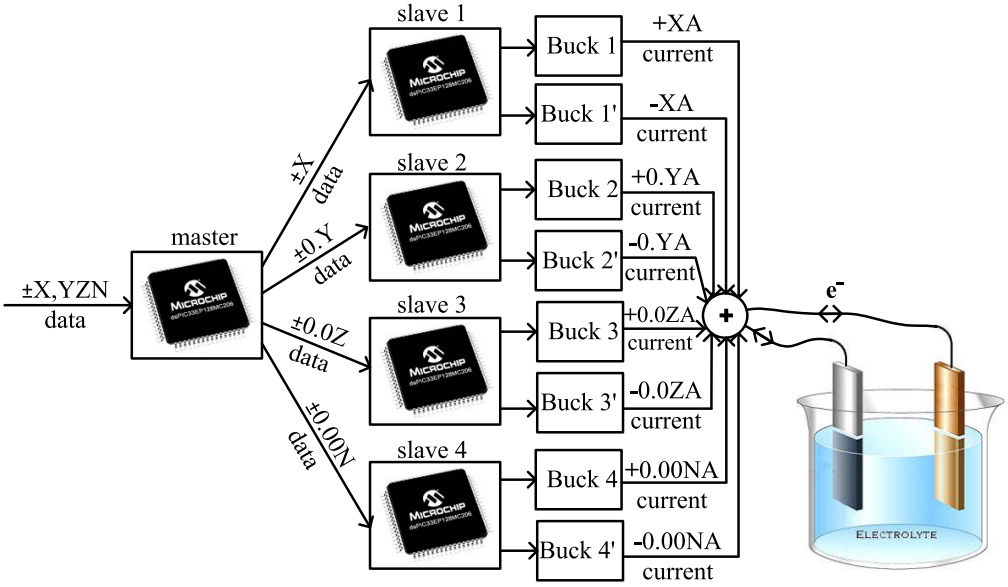

FIGURE 3. Dividing the current reference value into four values.

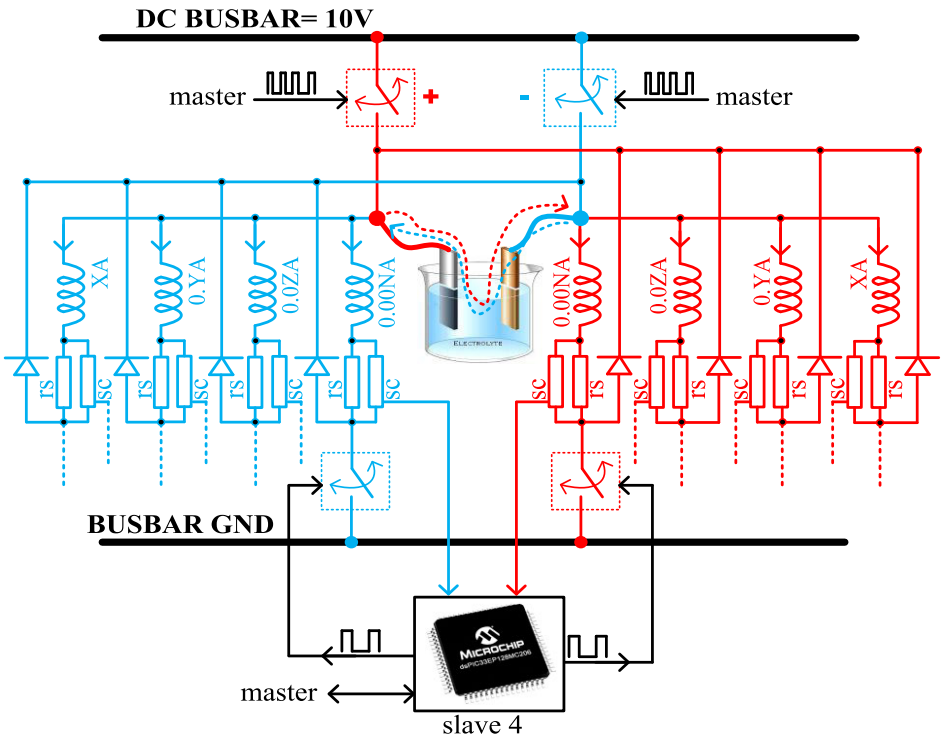

FIGURE 4. H-bridge, Buck Converter and slave processor connection.

Busbar voltage is the power supply indicated by Vdc, Figure 2. The switch is a suitable semiconductor that can provide energy transmission and cutting with a certain frequency. Coil and capacitor are passive electronic circuit components that filter the square voltage wave formed at the switching output and ensure the uninterrupted voltage on the Rload. Here, Rload represents the electrical resistance of the electrolyte, Figure 1.

The operating current of the current generator is between +9,999 and −9,999 amps. Current sensitivity is 0.001 amps. The ratio between the reference current and the current produced is less than 1%. In the generator system, a total of 8 Buck Converters were used, 4 for positive current waves and 4 for negative current waves. One embedded system is used for 2 Buck Converters. These embedded systems are qualified as slaves. 4 slave processors were used for 8 Buck Converter. One master processor was used to control these 4 slave processors. The master processor is responsible for dividing the current reference information sent by the PC software into 4 parts and transferring them to the slave processors, Figure 3.

The purpose of sending reference current information in this way is to increase the sensitivity of current control.

Not all current waveforms can be created with just one Buck Converter circuit structure. This is due to the Buck Converter output voltage unable to receive a negative value. If a negative voltage cannot be created on the Rload, a negative current that will pass through the Rload naturally cannot also occur, either. H-Bridge, a Power Electronics circuit topology, was used to generate negative voltage on the Rload. Therefore, in this study, H-Bridge and Buck Converter circuit topologies are fused with each other, Figure 4.

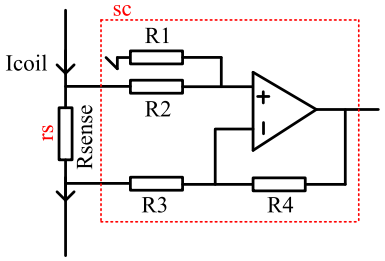

FIGURE 5. Current to voltage converter (sc).

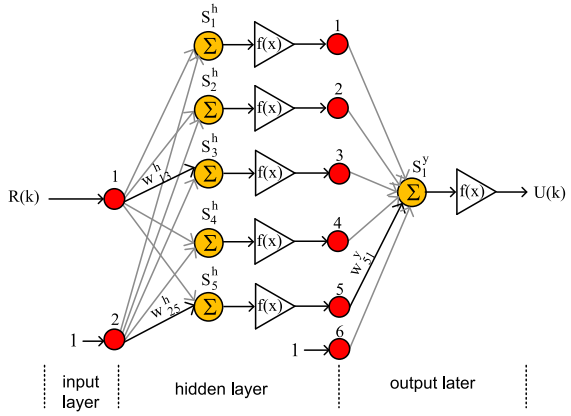

FIGURE 6. Structure of ANN.

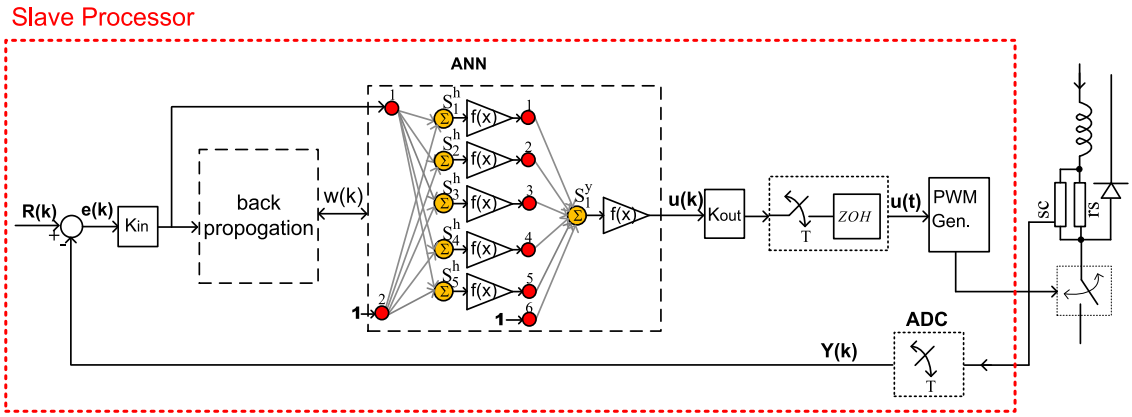

FIGURE 7. ANN-Buck Converter closed loop control block circuit.

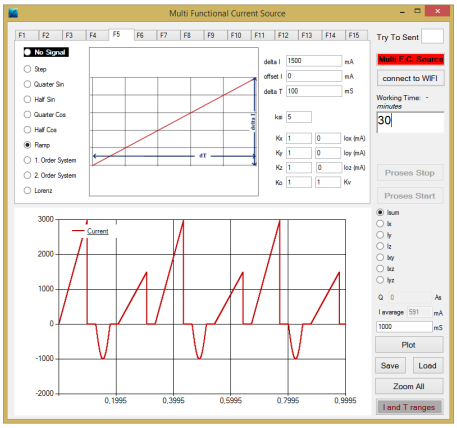

FIGURE 8. Developed software.

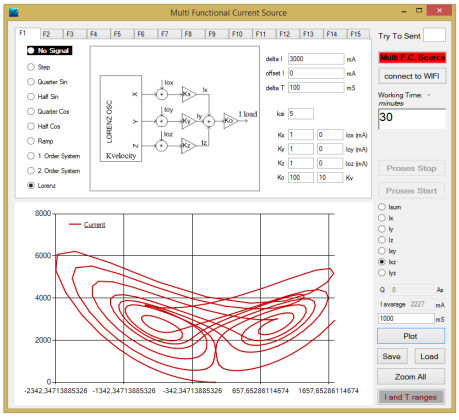

FIGURE 9. Current, selected to be Lorenz waves.

The switches included in the circuit can be selected from the BJT transistor, FET or IGBT family. Due to the low bus voltage and low electrolyte current, suitable semiconductors from the FET family (IXTN79N20) were selected in this study. Low-value resistors (rs) connected in series to the coils convert the coil current passing through the

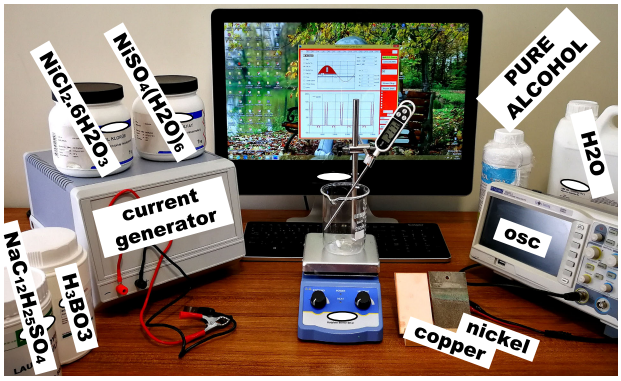

FIGURE 10. Materials of the coating process.

line into voltage, (1). Rsense=0.1ohm for 1-9A line, 1ohm for 0.1-0.9A line, 10ohm for 0.01-0.09A line and 100ohm for 0.001-009A line. The voltage formed on the resistor is transferred to the slave processor after it is processed by the operational processor circuit (sc), Figure 5.

It is quantified as positive current if the electric current flows over the red lines and negative current when it flows over the blue lines, Figure 4. Note that Buck Converter capacitors are not added to the hybrid circuit. The reason for this is that the circuit current is constantly changing. Since the current exchange rate is in a wide band range, it will narrow this band gap of the capacitor to be added. Therefore, the capacitor of the Buck Converter circuit is not used in this hybrid circuit system.

B. EMBEDDED SYSTEM

The embedded system was implemented using 5 dsPIC33 EP128MC206 microcontrollers, Figure 3. The bus of these processors is 16 bits and the processing capacity is 70MIPS. One of the processors that make up the embedded system is arranged to be master and the remaining 4 to be slave. The master receives the current parameters from the PC and transmits it periodically to the slave processors. Each

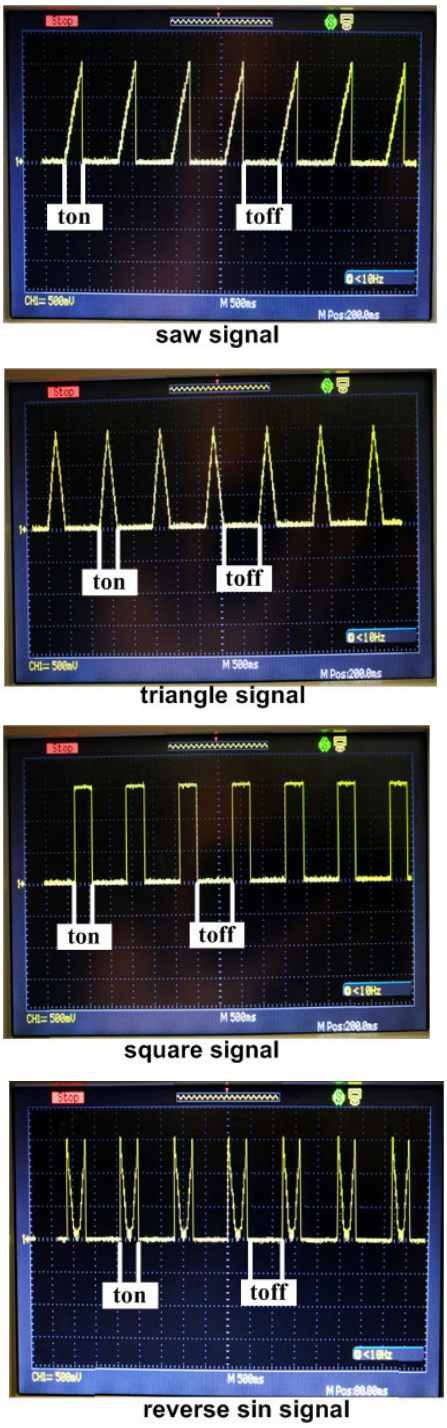

FIGURE 11. Selected current amplitudes and waveforms.

slave processor takes the Buck Converter circuit, which it is responsible for, based on the current reference information received from the master processor, Figure 3.

C. ANN BASED CURRENT CONTROL

ANN is a nonlinear adaptive mathematical algorithm based on error minimization. For this reason, it has been used effectively in the solution of various engineering problems. Studies related to ANN can be gathered in separate clusters in the form of classification, modeling, estimation and control in general, [31]–[37].

TABLE 1. Units for magnetic properties.

Parameters	Values
NiSO4·6H2O (nickel sulfate)	300g/L
NiCl2·6H2O (nickel chloride)	50g/L
H3BO3 (boric acid)	40g/L
SDS (sodium dodecyl sulfate)	0.2g/L
Temperature (◦C)	50±3
Substrate	Copper plate
pH	4±0.5
Current density	5A/dm^2
Anode	Nickel plate
Magnetic stirring (rpm)	300

ANN is structurally simple, Figure 6.

Variables in Figure 6 are described as,

$S_1^h, S_2^h, .., S_5^h$: Addition centers of hidden (h) layer

$w_{11}^h, w_{12}^h, .., w_{15}^h$: Weights between ANN input and hidden layer addition centers

$w_{21}^h, w_{22}^h, .., w_{25}^h$: Weights, between bias input and hidden layer addition centers, belong to input layer

$R\,(k)$: ANN input

$U\,(k)$: ANN output

S_1^y: Addition centre of ANN output layer

$w_{11}^y, w_{21}^y, \ldots, w_{51}^y$: Weights between output of hidden layer and output layer addition centre of ANN

w_{61}^y: Weight between bias input of output layer and addition centre of output layer

$f\,(x)$: Activation function

ANN completes the calculation cycle in 2 rounds. In the first round, it updates the weights based on the difference between input and output. In the second round, using input data it produces a result, i.e. output data, through mathematical expressions, [37].

In the current generator system, ANN monitors Buck Converter hardware. Its task is to minimize the difference between the reference current and the current that will pass through the Buck Converter circuit.

The ANN algorithm has become a discrete time, nonlinear, optimal, adaptive control algorithm for these operating conditions. In order to realize this transformation, parameters of ANN algorithm should be optimized [38]. However, after this optimization, ANN can be converted to the targeted control algorithm. The ANN algorithm, the software of which is realized in slave processors, and the closed loop control block diagram realized with Buck Converter is given in Figure 7.

D. PC SOFTWARE

PC software is a product that can be run in any Microsoft platform and can exchange data with the current generator system. It was developed specifically for this study, Figure 8. The communication protocol between the PC software and

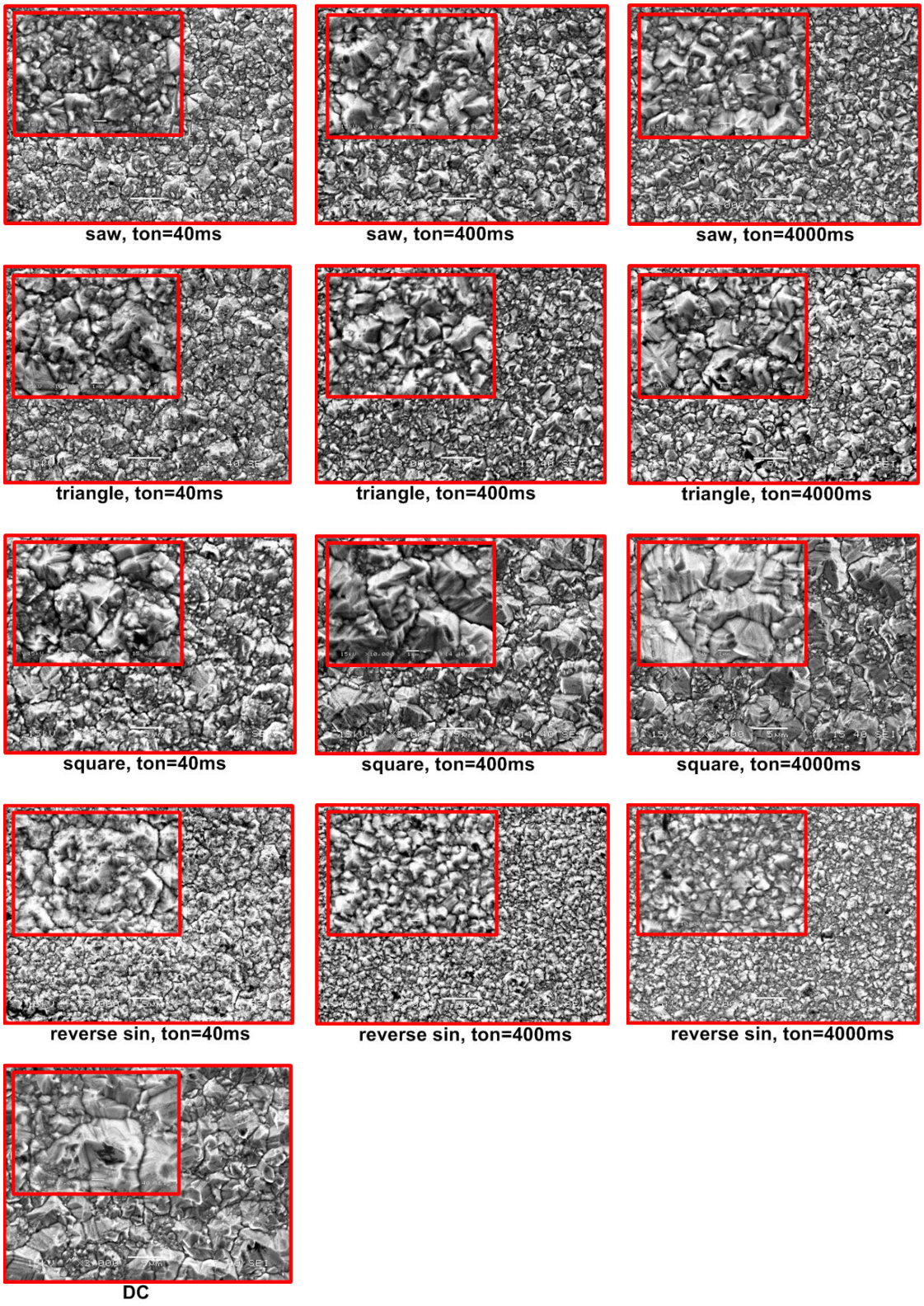

FIGURE 12. Surface coating results for Experiment 1. SEM parameters are 15kV/x3000 and 15kV/x10000.

the current generator hardware has been found suitable for use as WiFi. Thus, high-reliability data transfer is made possible.

PC software is the environment where the coating current is shaped by the user. Here, amplitude, shape and period of the coating current are determined by the user. A period can consist of 15 different parts. For example, the above 1 period current waveform is composed of 6 parts, Figure 8.

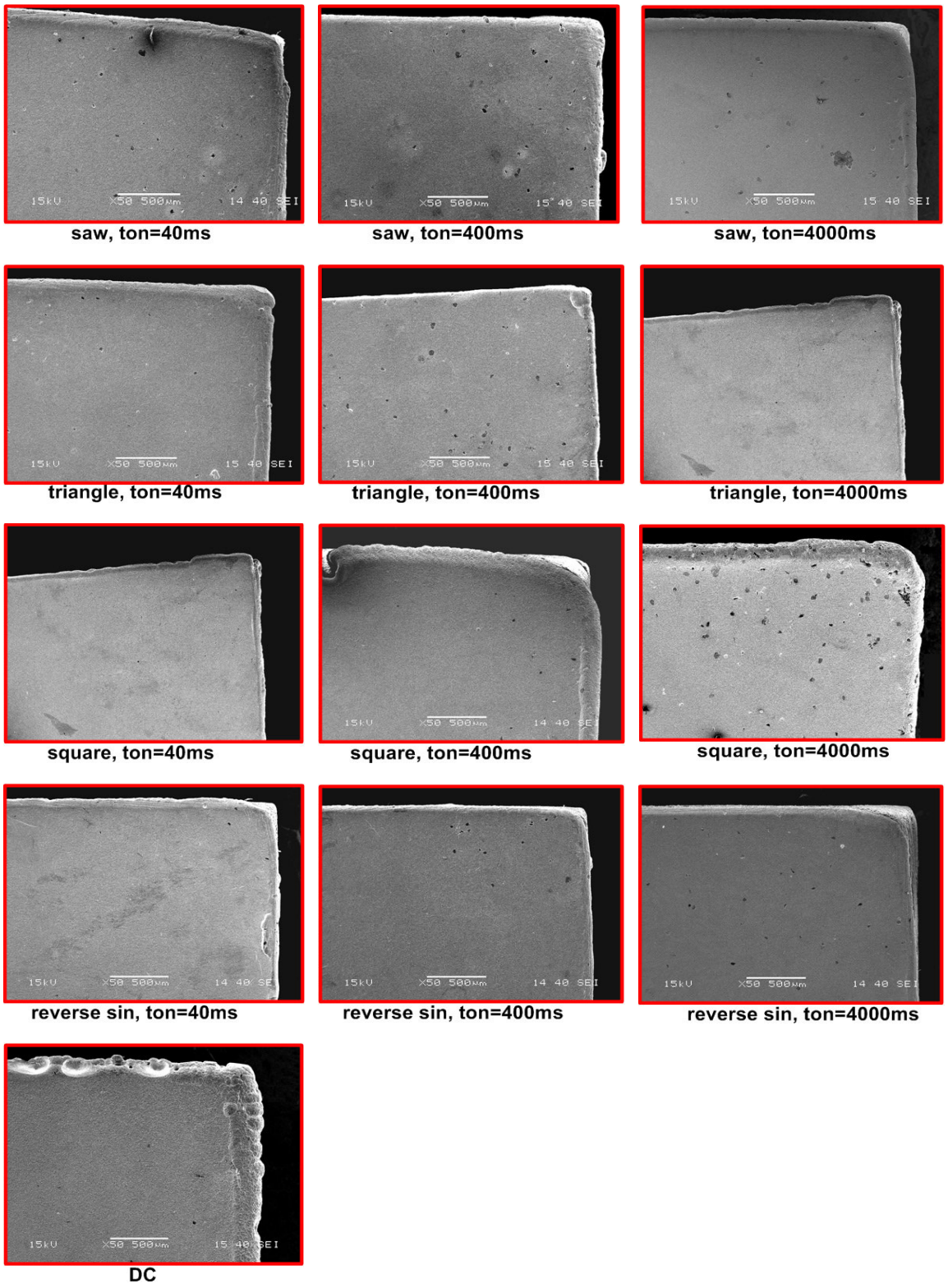

FIGURE 13. Corner coating results. SEM parameters, 15kV/x50.

A periodic current wave can be constructed in 8 different waveforms: step, quarter sinus, half sinus, quarter cosine, half cosine, ramp, 1st degree and 2nd degree system output curves used in control engineering, Figure 8. In addition, Lorenz nonlinear chaotic signals in the science of Chaos can also be converted into current waveform, Figure 9. In this waveform,

the user can change the amplitude and rate of change of the current wave, too.

The hardware that runs the ANN is the embedded system. The ANN algorithm is coded into each of the slave processors. The output value obtained from the ANN algorithm is converted to the appropriate duty values via the PWM generator located in the slave processor and then applied to the gate element in the form of a pulse train.

III. EXPERIMENTAL RESULTS

Nickel plating work on copper has two different experimental processes, Figure 10. In the first experiment process, the electric current passing through the electrolyte does not get negative values, while in the second experiment process it gets negative values.

Coating parameters used for both experimental processes are given in the table below.

A. COATING EXPERIMENT 1

In this study, coating experiment was carried out using four different current waves with variable current, named Saw, Triangle, Square and Inverse Half Sine, Figure 11. The coating successes of these current waves are discussed by comparing the coating results obtained using the traditional method DC current.

In the coating process, the peak values of all current signals were fixed at 1500mA. Each current wave except DC was produced in 3 different time rate of change with ton = 40ms and toff = 80ms, ton = 400ms and toff = 800ms with ton = 4000ms and toff = 8000ms, Figure 11. After the coating process, surface and corner coating successes were observed and discussed, Figure 12 and 13. On the coating process each coating experiment had been limited to 30 minutes.

Today, the Electrodeposition method used in the field of metallurgy and materials engineering is based on ''pulse'' and generally the results of the experiment are compared with ''DC'' current performed under the same conditions. However, if the coated surfaces obtained in experiment 1 are examined, it will be seen that the morphology of the coated surfaces obtained by using ''DC'' and ''Pulse'' currents are close to each other, Figure 12. And in both current coating methods, the surfaces are large grain size and the surface of the coated material is quite rough.

Material surfaces coated with current waveforms other than ''DC'' and ''Pulse'' current method have a finer grain size and appear to have a lower rough surface, figure 12. Especially with ''Reverse Half Sine'' current wave is seen that the surface of the material coated has the best grain size and the distribution is more homogeneous. It is seen that the most successful of the 3 experiments performed using different parameter ''Inverse Half Sine'' current wave is the coating experiment performed for ton = 400ms.

The surfaces obtained from the coating experiments carried out using the ''Saw'' and ''Triangular'' current waveforms appear to be smoother surface than the ''Pulse'' method, Figure 12. In the ''Saw'' current method, due to the sudden drop of current, it has a rougher coating surface than the surface covered with ''Triangle'' current wave.

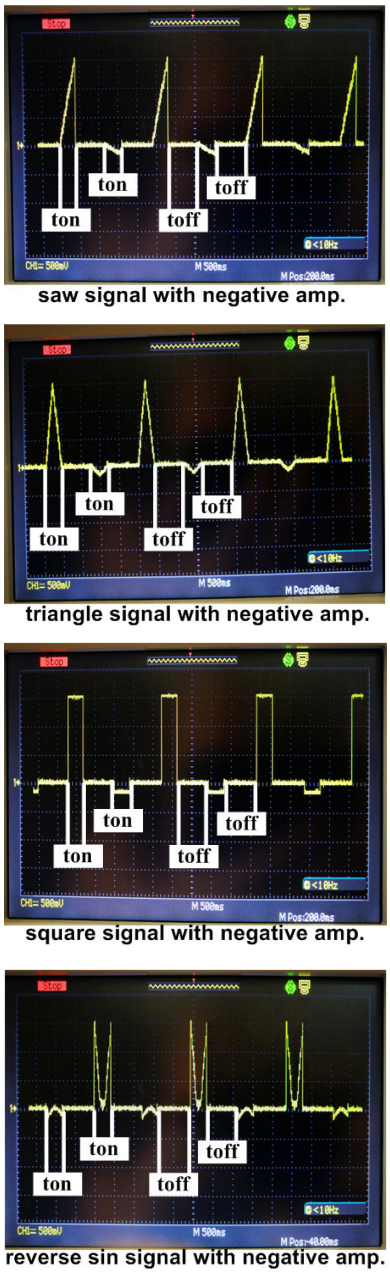

FIGURE 14. Current waveforms used in the coating process.

A troubled parameter of the coating process is the success of covering the corners. Corners have high tension area because they are pointed areas. Due to this high voltage area, the corners are covered more intensely. Therefore, in industrial environment, materials with pointed corners are given to grinding after coating. The purpose of the grinding process is to eliminate the deformation caused by the covering material. This process causes time and energy losses. It causes scratches on the coating surface.

The corner coating results obtained in the frame of Experiment 1 is reflected in Figure 13. As can be seen, the smoothest

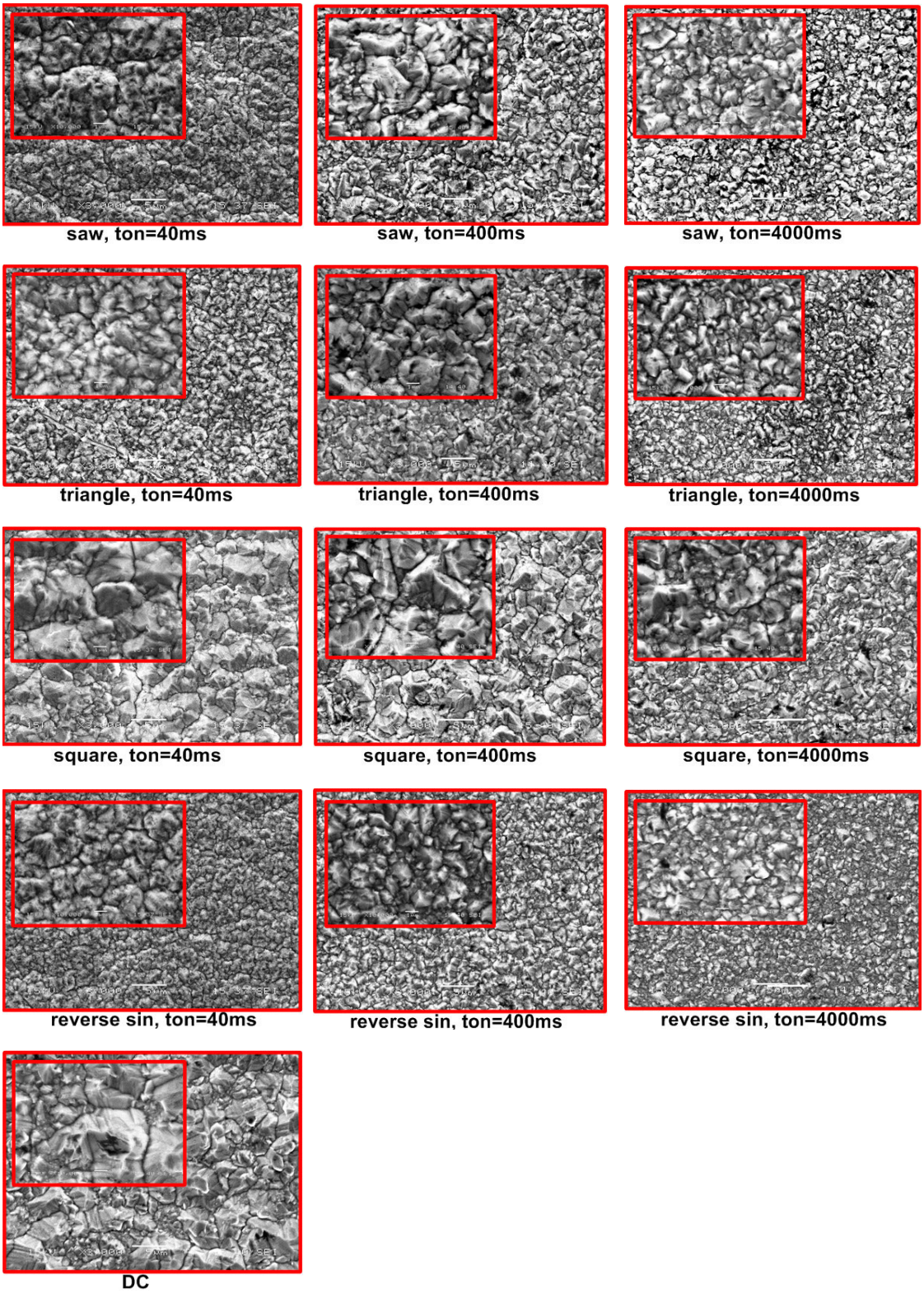

FIGURE 15. Surface coating results. SEM parameters are 15kV/x3000 and 15kV/x10000.

corner coating still belongs to the ''Inverse Half Sinus'' coating process. The worst corner coating belongs to the coating method performed with ''DC'' current followed by ''Pulse'' current. In the coating process, the current waveform, which advances corner coatings at the same height and roughness as the surface, was again ''Inverse Half Sine''. It has been

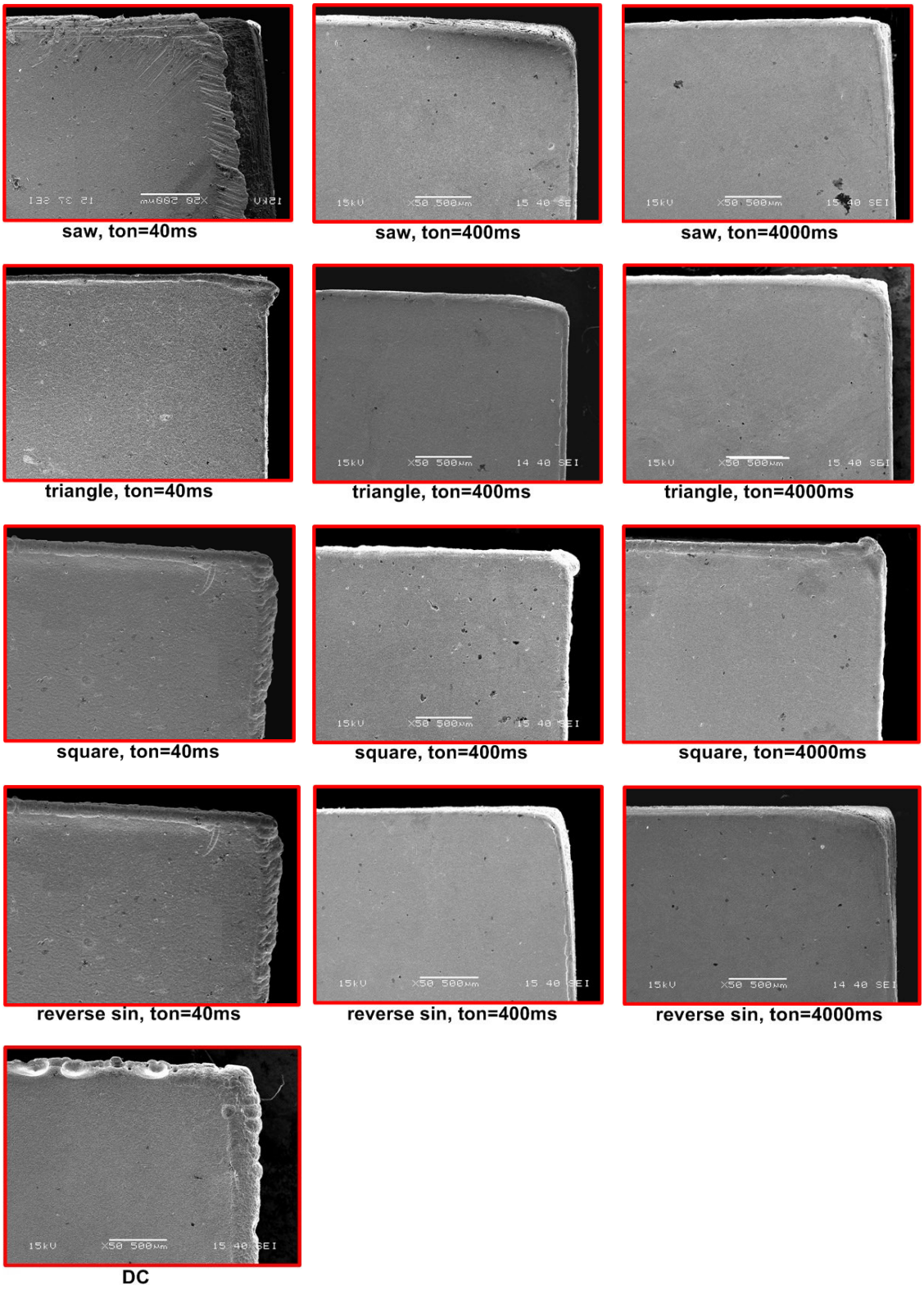

FIGURE 16. Corner coating results. SEM parameters, 15kV/x50.

observed that selecting the ton parameter of "Inverse Half Sine" for this coating experiment 400ms best affects the coating.

B. COATING EXPERIMENT 2

In this study, coating experiment was carried out using four different current waves with variable current, named Saw,

Triangle, Pulse and Inverse Half Sine, Figure 14. Unlike the previous experiment, coating currents have negative current values. The negative amplitude values of the current signals were chosen to be 150mA, which is 10% of the positive amplitude value. The purpose of this experiment is to reveal possible changes in the final coating quality of some dissolution are achieved in the coating process. Coating successes of these current waves are discussed by comparing the coating results obtained using the traditional method DC current. In this study, the coating time had been limited to 30 minutes again.

Coating surfaces containing negative flow have been observed to have a fine-grain structure as shown in Figure 15. In terms of surface grain size, the best result, perhaps the perfect result was obtained using the ''Inverse Half Sinus'' current waveform. Especially for the ''ton'' parameter value 400ms, the material surface is very smooth.

Again, the ''DC'' and ''Pulse'' current method failed more in surface morphology than other coating results. Because the roughest and heterogeneous dispersion was observed on the material surfaces covered with these two types of current. The surfaces obtained from the coating experiments carried out using the ''Saw'' and ''Triangular'' current waveforms, on the other hand, formed very similar surfaces, Figure 15.

When the covering performances of corners and edges are examined, it is seen that ''Reverse Half Sinus'' has by far the best covering edge and corner as shown in Figure 16. Again, it is understood that the ''Inverse Half Sine'' for the ''ton'' parameter value 400ms performs the most optimal coating.

IV. CONCLUSIONS

Since the waveforms that can be produced by the electrical current sources used in coating science are limited, studies have been constantly stuck around ''DC'', ''Pulse'' and ''Pulse Riverse'' current waveforms. Although ''Pulse'' based studies are tried to be diversified by changing the number and amplitude values of the pulse sequences, as a result, coating studies cannot exceed these 3 current types. However, in engineering and mathe-matics, many functions and their output waveforms are derived. In this study, coating experiment had been carried out by using different current waveforms outside these 3 well known current waves. Before the coating experiment, we proposed that if the shape of current waves is increased, traditional current types will not be needed to be produced and used in different numbers and amplitudes anymore. As a matter of fact, all experimental results showed that when currents with different type of function are used outside of ''DC'', ''Pulse'' and ''Pulse Reverse'', coating surfaces have been much more successfully coated.

V. PROPOSAL

In future studies, the most suitable current waveform can be investigated in the field of coating by scanning various disciplines. A richer range of experiments can be created for coating studies by classifying current waveforms under the headings of linear-nonlinear, periodic-non periodic, animal sounds and nature sounds. Going a little further, the effects of current waves based on music genres on the coating can be studied. Finally, we may also suggest that, by increasing the number of anode material to be used in the coating process, current with different function waveforms can be applied for each anode. Thanks to this coating method, the coating quality can be further improved, since each current waveform will have its own improved coating parameter.

REFERENCES

[1] S. Mbugua Nyambura, M. Kang, J. Zhu, Y. Liu, Y. Zhang, and N. J. Ndiithi, ''Synthesis and characterization of Ni–W/Cr_2O_3 nanocomposite coatings using electrochemical deposition technique,'' *Coatings*, vol. 9, no. 12, p. 815, Dec. 2019, doi: 10.3390/coatings9120815.

[2] V. Torabinejad, M. Aliofkhazraei, S. Assareh, M. H. Allahyarzadeh, and A. S. Rouhaghdam, ''Electrodeposition of ni-fe alloys, composites, and nano coatings—A review,'' *J. Alloys Compounds*, vol. 691, pp. 841–859, Jan. 2017, doi: 10.1016/j.jallcom.2016.08.329.

[3] S. Mahdavi and S. R. Allahkaram, ''Composition, characteristics and tribological behavior of cr, Co–cr and Co–cr/TiO_2 nanocomposite coatings electrodeposited from trivalent chromium based baths,'' *J. Alloys Compounds*, vol. 635, pp. 150–157, Jun. 2015, doi: 10.1016/j.jallcom.2015.02.119.

[4] T. Borkar and S. P. Harimkar, ''Effect of electrodeposition conditions and reinforcement content on microstructure and tribological properties of nickel composite coatings,'' *Surf. Coat. Technol.*, vol. 205, nos. 17–18, pp. 4124–4134, May 2011, doi: 10.1016/j.surfcoat.2011.02.057.

[5] C.-K. Chung and W.-T. Chang, ''Electrochemical deposition and mechanical property enhancement of the nickel and nickel-cobalt films,'' in *Handbook of Manufacturing Engineering and Technology*, A. Y. C. Nee, Ed. London, U.K.: Springer, 2015, pp. 2891–2927.

[6] S. Spanou and E. A. Pavlatou, ''Pulse electrodeposition of Ni/nano-TiO_2 composites: Effect of pulse frequency on deposits properties,'' *J. Appl. Electrochem.*, vol. 40, no. 7, pp. 1325–1336, Jul. 2010, doi: 10.1007/s10800-010-0080-3.

[7] M. Srivastava, V. K. W. Grips, and K. S. Rajam, ''Electrochemical deposition and tribological behaviour of ni and Ni–Co metal matrix composites with SiC nano-particles,'' *Appl. Surf. Sci.*, vol. 253, no. 8, pp. 3814–3824, Feb. 2007, doi: 10.1016/j.apsusc.2006.08.022.

[8] M. E. Estrada, ''Model-based framework for alloy electrodeposition processes,'' Univ. Tulsa, Tulsa, OK, USA, Tech. Rep., 2008.

[9] D. S. Jayakrishnan, ''Electrodeposition: The versatile technique for nanomaterials,'' in *Corrosion Protection and Control Using Nanomaterials*. Amsterdam, The Netherlands: Elsevier, 2012, pp. 86–125.

[10] D. Melciu and N. Maidee, ''Pulse-electroplating: Process parameters and their influence on the formed microstructure,'' Chalmers Univ. Technol., Gothenburg, Sweden, Tech. Rep., 2010.

[11] A. Boukhouiete and J. Creus, ''Nickel deposits obtained by continuous and pulsed electrodeposition processes,'' *J. Mater. Environ. Sci.*, vol. 6, no. 7, pp. 1840–1844, 2015.

[12] A. Balasubramanian, D. S. Srikumar, G. Raja, G. Saravanan, and S. Mohan, ''Effect of pulse parameter on pulsed electrodeposition of copper on stainless steel,'' *Surf. Eng.*, vol. 25, no. 5, pp. 389–392, Jul. 2009, doi: 10.1179/026708408X344680.

[13] T. Borkar, ''Electrodeposition of nickel composite coatings,'' Mumbai Univ., Mumbai, India, Tech. Rep., 2010.

[14] A. M. El-Sherik and U. Erb, ''Synthesis of bulk nanocrystalline nickel by pulsed electrodeposition,'' *J. Mater. Sci.*, vol. 30, no. 22, pp. 5743–5749, Nov. 1995, doi: 10.1007/BF00356715.

[15] M. S. Chandrasekar and M. Pushpavanam, ''Pulse and pulse reverse plating—Conceptual, advantages and applications,'' *Electrochimica Acta*, vol. 53, no. 8, pp. 3313–3322, Mar. 2008, doi: 10.1016/j.electacta.2007.11.054.

[16] L. M. Chang, M. Z. An, and S. Y. Shi, ''Microstructure and characterization of ni-Co/Al_2O_3 composite coatings by pulse reversal electrodeposit,'' *Mater. Chem. Phys.*, vol. 100, nos. 2–3, pp. 395–399, Dec. 2006, doi: 10.1016/j.matchemphys.2006.01.035.

[17] P. Gyftou, E. A. Pavlatou, and N. Spyrellis, "Effect of pulse electrodeposition parameters on the properties of Ni/nano-SiC composites," *Appl. Surf. Sci.*, vol. 254, no. 18, pp. 5910–5916, Jul. 2008, doi: 10.1016/j.apsusc.2008.03.151.
[18] L. M. Chang, D. Chen, J. H. Liu, and R. J. Zhang, "Effects of different plating modes on microstructure and corrosion resistance of Zn–Ni alloy coatings," *J. Alloys Compounds*, vol. 479, nos. 1–2, pp. 489–493, Jun. 2009, doi: 10.1016/j.jallcom.2008.12.108.
[19] R. M. Reddy, B. M. Praveen, K. G. Chandrappa, and K. O. Nayana, "Generation of Ni–Si3N4nanocomposites by DC, PC and PRC electrodeposition methods," *Surf. Eng.*, vol. 32, no. 7, pp. 501–507, Jul. 2016, doi: 10.1080/02670844.2016.1148323.
[20] W. A. Aperador Chaparro and E. V. Lopez, "Electrodeposition of nickel plates on copper substrates using PC y PRC," *Matéria (Rio de Janeiro)*, vol. 12, no. 4, pp. 583–588, Dec. 2007, doi: 10.1590/S1517-70762007000400006.
[21] S. Imanian Ghazanlou, A. Shokuhfar, S. Navazani, and R. Yavari, "Influence of pulse electrodeposition parameters on microhardness, grain size and surface morphology of Ni–Co/SiO_2 nanocomposite coating," *Bull. Mater. Sci.*, vol. 39, no. 5, pp. 1185–1195, Sep. 2016, doi: 10.1007/s12034-016-1256-1.
[22] S.-C. Chang, J.-M. Shieh, B.-T. Dai, and M.-S. Feng, "Investigations of pulse current electrodeposition for damascene copper metals," *J. Vac. Sci. Technol. B, Microelectron. Nanometer Struct.*, vol. 20, no. 6, p. 2295, 2002, doi: 10.1116/1.1518974.
[23] D. D. Shreeram, S. Li, V. Bedekar, H. Cong, and G. L. Doll, "Effect of reverse pulse time on electrodeposited Ni-W coatings," *Surf. Coat. Technol.*, vol. 325, pp. 386–396, Sep. 2017, doi: 10.1016/j.surfcoat.2017.06.037.
[24] P. Kamnerdkhag, M. L. Free, A. A. Shah, and A. Rodchanarowan, "The effects of duty cycles on pulsed current electrodeposition of Zn Ni Al_2O_3 composite on steel substrate: Microstructures, hardness and corrosion resistance," *Int. J. Hydrogen Energy*, vol. 42, no. 32, pp. 20783–20790, Aug. 2017, doi: 10.1016/j.ijhydene.2017.06.049.
[25] I. Matsui and N. Omura, "Comparison of tensile properties of bulk nanocrystalline Ni–W alloys electrodeposited by direct, pulsed, and pulsed-reverse currents," *Mater. Trans.*, vol. 59, no. 1, pp. 123–128, 2018, doi: 10.2320/matertrans.M2017256.
[26] J. Wojciechowski, M. Baraniak, J. Pernak, and G. Lota, "Nickel coatings electrodeposited from watts type baths containing quaternary ammonium sulphate salts," *Int. J. Electrochem. Sci.*, vol. 12, pp. 3350–3360, Apr. 2017, doi: 10.20964/2017.04.70.
[27] M. Hagarová, D. Jakubéczyová, and J. Cervová, "Microstructure and properties of electroplated Ni-Co alloy coatings," *Int. J. Electrochem. Sci.*, vol. 10, p. 7, doi:2015.
[28] N. S. Qu, D. Zhu, K. C. Chan, and W. N. Lei, "Pulse electrodeposition of nanocrystalline nickel using ultra narrow pulse width and high peak current density," *Surf. Coat. Technol.*, vol. 168, nos. 2–3, pp. 123–128, May 2003, doi: 10.1016/S0257-8972(03)00014-8.
[29] G. Mühürcü, E. Köse, A. Muhurcu, and M. Özdemir, "PI parameter optimization by fairly algorithm for optimal controlling of a buck Converter's output state variable," *Sakarya Univ. J. Sci.*, vol. 22, no. 5, pp. 1267–1273, Sep. 2018, doi: 10.16984/saufenbilder.327296.
[30] E. Köse, A. Mühürcü, G. Mühürcü, and E. Aydoğan, "PI parameter optimization by using ant colony algorithm for optimal controlling of a buck converter's output voltage," *J. Fac. Eng. Archit.*, vol. 32, no. 4, pp. 153–162, 2017.
[31] M. A. Beg, M. K. Khedkar, S. R. Paraskar, and G. M. Dhole, "Feed-forward artificial neural network–discrete wavelet transform approach to classify power system transients," *Electr. Power Compon. Syst.*, vol. 41, no. 6, pp. 586–604, Apr. 2013.
[32] O. Erkaymaz, M. Özer, and N. Yumuşak, "Impact of small-world topology on the performance of a feed-forward artificial neural network based on 2 different real-life problems," *Turkish J. Electr. Eng. Comput. Sci.*, vol. 22, pp. 708–718, Apr. 2014.
[33] M. Zounemat-Kermani, O. Kisi, and T. Rajaee, "Performance of radial basis and LM-feed forward artificial neural networks for predicting daily watershed runoff," *Appl. Soft Comput.*, vol. 13, no. 12, pp. 4633–4644, 2013.
[34] V. Nabiyev and Y. Zeka, 1st ed. Istanbul, Turkey: Seçkin, 2012.
[35] P. Deepa and R. Sivakumar, "Synthesis of heuristic control strategies for liquid level control in spherical tank," in *Proc. 3rd Int. Conf. Adv. Electr., Electron., Inf., Commun. Bio-Inform. (AEEICB)*, Chennai, India, Feb. 2017, pp. 27–28.
[36] L. Ma, P. Cao, Z. Gao, and K. Y. Lee, "ANN and PSO based intelligent model predictive optimal control for large-scale supercritical power unit," in *Proc. IEEE Int. Conf. Inf. Autom. (ICIA)*, Ningbo, China, Aug. 2016, pp. 1–3.
[37] X. Lin, A. Li, and W. Zhang, "Application of PSO-based ANN in knowledge acquisition for the selection of optimal milling parameters," in *Proc. 6th World Congr. Intell. Control Autom.*, Dalian, China, 2006, pp. 21–23.
[38] A. Mühürcü, "FFANN optimization by ABC for controlling a 2nd order SISO system's output with a desired settling time," *Processes*, vol. 7, no. 1, p. 4, Dec. 2018, doi: 10.3390/.pr7010004.

GÜLÇIN MÜHÜRCÜ was born in Mersin, Turkey, in 1981. She received the B.S. and M.S. degrees in mechanical engineering from Sakarya University, Turkey, in 2004 and 2010, respectively. She has been a Lecturer with the Control and Automation Technology Department, Kırklareli University, since 2017.

MUSTAFA KEMAL KÜLEKCI received the Ph.D. degree from Gazi University, Ankara, Turkey, in 2000. He is currently a Professor with the Department of Mechanical Engineering, Faculty of Engineering, Tarsus University, Turkey. His research interests include nontrditinal manufacturing process, advanced manufacturing processes, mechanical properties of metallic materials, and forming of mettallic materials.